Research Article

Cancer Immunology Research

An Anticancer Drug Cocktail of Three Kinase Inhibitors Improved Response to a Dendritic Cell–Based Cancer Vaccine

Jitao Guo[1], Elena Muse[1], Allison J. Christians[1], Steven J. Swanson[2], and Eduardo Davila[1,3,4]

Abstract

Monocyte-derived dendritic cell (moDC)–based cancer therapies intended to elicit antitumor T-cell responses have limited efficacy in most clinical trials. However, potent and sustained antitumor activity in a limited number of patients highlights the therapeutic potential of moDCs. *In vitro* culture conditions used to generate moDCs can be inconsistent, and moDCs generated *in vitro* are less effective than natural DCs. On the basis of our study highlighting the ability for certain kinase inhibitors to enhance tumor antigenicity, we therefore screened kinase inhibitors for their ability to improve DC immunogenicity. We identified AKT inhibitor MK2206, DNA-PK inhibitor NU7441, and MEK inhibitor trametinib as the compounds most effective at modulating moDC immunogenicity. The combination of these drugs, referred to as MKNUTRA, enhanced moDC activity over treatment with individual drugs while exhibiting minimal toxicity. An evaluation of 335 activation and T-cell–suppressive surface proteins on moDCs revealed that MKNUTRA treatment more effectively matured cells and reduced the expression of tolerogenic proteins as compared with control moDCs. MKNUTRA treatment imparted to ICT107, a glioblastoma (GBM) DC-based vaccine that has completed phase II trials, an increased ability to stimulate patient-derived autologous $CD8^+$ T cells against the brain tumor antigens $IL13R\alpha2_{(345\text{-}354)}$ and $TRP2_{(180\text{-}188)}$. *In vivo*, treating ICT107 with MKNUTRA, prior to injection into mice with an established GBM tumor, reduced tumor growth kinetics. This response was associated with an increased frequency of tumor-reactive lymphocytes within tumors and in peripheral tissues. These studies broaden the application of targeted anticancer drugs and highlight their ability to increase moDC immunogenicity.

Introduction

Dendritic cells (DC) are professional antigen-presenting cells with the capacity to activate tumor-reactive T cells. DC-based cancer therapies received FDA approval in 2010. The objective response rates to DC vaccines hover around 15% and are associated with increased T-cell activity and tumor infiltration (1). Although most responses to DC-based vaccines were incomplete, the strong responses observed in a subset of patients merit further investigation into the mechanisms that support the generation of robust and durable T-cell activity. The failure to elicit sustained antitumor T-cell responses in patients with cancer has been attributed to a variety of reasons including the poor immunogenicity of DC vaccines as well as the expression of T-cell–inhibitory signals such as programmed death ligand 1 (PD-L1) and PD-L2 (2, 3).

Initial studies focused on developing *in vitro*–based monocyte-derived DCs (moDC) with the ability to activate $CD8^+$ T-cell responses. moDCs are generally matured and activated in the presence of a cocktail of cytokines and "danger signals," including TNFα and Toll-like receptor (TLR) agonists. Although many *in vitro*–differentiated moDCs can be generated, their differentiation state and function remain in doubt. For example, moDCs are usually differentiated with GM-CSF and IL4 (4), which do not drive differentiation of natural DCs. The altered *in vitro* differentiation protocol could result in altered DC phenotype and function (5, 6). Also, depending upon the cues received by DCs *in vivo*, they can differentiate into specialized subsets garnering the ability to mediate distinct immune responses (7). On the other hand, *in vitro*–generated moDCs appear to be more heterogenous than natural DCs in terms of functional capacities and *in vivo* migration patterns (8, 9). Suboptimal differentiation conditions can result in the generation of immature or semimature moDCs that can be tolerogenic (10). The frequency and differentiation of moDCs under standardized manufacturing procedures varies across patients. Nevertheless, ongoing strategies are focused on improving the quality of moDC-based vaccines by combining them with other immunotherapies including checkpoint blockade–based therapies or by refining their properties to increase immunogenicity.

Variations of moDC maturation cocktails have been investigated and are typically composed of inflammatory cytokines, TLR agonists, CD40 agonists, and/or prostaglandin E_2 (PGE_2; ref. 11). However, these receptors can become saturated, and responses

[1]Division of Medical Oncology, Department of Medicine, University of Colorado, Anschutz Medical Campus, Aurora, Colorado. [2]ImmunoCellular Therapeutics, Ltd., Westlake Village, California. [3]Human Immunology and Immunotherapy Initiative, University of Colorado, Anschutz Medical Campus, Aurora, Colorado. [4]University of Colorado Comprehensive Cancer Center, Aurora, Colorado.

Note: Supplementary data for this article are available at Cancer Immunology Research Online (http://cancerimmunolres.aacrjournals.org/).

Corresponding Author: Eduardo Davila, University of Colorado Anschutz Medical Campus, MS8117, 12801 East 17th Avenue, Aurora, CO 80045. Phone: 303-724-0817; Fax: 303-724-3889; E-mail: eduardo.davila@ucdenver.edu

Cancer Immunol Res 2019;7:1523–34

doi: 10.1158/2326-6066.CIR-18-0684

may plateau (12). Potentiation of the effects of these factors could improve moDC maturation and immunogenicity. Alternatively, moDCs can be genetically engineered to improve efficacy (13), although such modifications add to the already labor-intensive process required to generate moDC cells.

Most receptor–ligand interactions transduce signals through kinase-mediated phosphorylation (14). Small-molecule kinase inhibitors have been developed for targeted anticancer therapy (15, 16). To date, 43 kinase inhibitors are approved worldwide. Clinical trials are testing more than 150 candidates, most of which are for cancer treatment (15). On the basis of our study, highlighting the ability of certain kinase inhibitors to enhance tumor immunogenicity, we screened a library of 60 kinase inhibitors and identified AKT, DNA-PK, and MEK inhibitors that increased the moDC immunogenic phenotype while decreasing expression of T-cell–inhibitory factors on moDCs. Combining MK2206, NU7441, and trametinib (MKNUTRA) further enhanced moDC immunogenic phenotype and function. We observed that MKNUTRA treatment of a glioblastoma multiforme (GBM) DC-based vaccine, known as ICT107 (17), which has completed a phase II clinical trial (NCT01280552), improved ICT107's ability to activate and expand tumor-reactive T cells and augmented antitumor activity in tumor-bearing mice. These findings shed insights into the immunomodulatory capacity of various small-molecule kinase inhibitors, broaden the application of these compounds, and highlight the opportunity to improve the efficacy of DC-based vaccines.

Materials and Methods

Reagents

Kinase inhibitors (Selleckchem) used in this study are listed in Supplementary Table S1. All drugs were dissolved in dimethyl sulfoxide (DMSO). AIM-V media (Invitrogen) was supplemented with 2.5% human AB serum (Sigma), penicillin–streptomycin (100 U/mL, Thermo Fisher Scientific), and 1% NEAA (Thermo Fisher Scientific). BioLegend products were listed as follows: PE/cy7 anti-human CD209 (330113), Brilliant Violet 605 anti-human HLA-A,B,C (311432), FITC anti-human HLA-DR, DP, DQ (361706), APC anti-human CD83 (305312), Pacific Blue anti-human CCR7 (353210), Percp/cy5.5 anti-human PD-L1 (329738), PE anti–PD-L2 (329606), Alexa Fluor 488 anti-human CD40 (334318), PE anti-human CD86 (374206), Brilliant Violet 605 anti-human CD3 (317322), PE/Cy7 anti-human CD8α (300914), recombinant human GM-CSF (572905), recombinant human IL4 (574008), recombinant human TNFα (570106), recombinant human IL6 (570804), recombinant human IL1β (579404), recombinant human IFNγ (570204), recombinant human IFNα (592704), recombinant human IL2 (589108), zombie aqua fixable viability kit (423101), LEGENDScreen human PE Kit (700007), LEGEND MAX human IFNγ ELISA Kit (430107), and LEGEND MAX human granzyme B ELISA Kit (439207). IL12p70 ELISA kit was from Thermo Fisher Scientific (BMS238HS). LPS (L4524), prostaglandin E2 (P0409), and polyinosinic–polycytidylic acid sodium salt (pI:C, P1530) were from Sigma. MART1 tetramer (NIH Tetramer Core Facility) and NY-ESO-1 pentamer (ProImmune) were used to track antigen-specific T cells. Antigen-loaded HLA-A2:Ig dimers were prepared according to the manufacturer's standard protocols (551263, BD Biosciences). Solvent-loaded HLA-A2:Ig dimers were prepared for analyzing background staining. HLA-A2–restricted peptide NY-ESO-$1_{(157\text{-}165)}$ [SLLMWITQV], Melan-A/MART$1_{(27\text{-}35)}$ [AAGIGILTV], GP$100_{(209\text{-}217)}$ [IMDQVPFSV], TRP$2_{(180\text{-}188)}$ [SVYDFFVWL], HER$2_{(773\text{-}782)}$ [VMAGVGSPYV], and IL13Rα$2_{(345\text{-}354)}$ [WLPFGFILI] were synthesized by Genscript.

Generation and phenotyping of human moDCs and DC vaccine preparation

Human moDCs were generated as described previously (18). Briefly, adherent cells from peripheral blood mononuclear cells (PBMC) were cultured in complete AIM-V media supplemented with GM-CSF (100 U/mL) and IL4 (200 U/mL) for 6 days and matured by LPS (1 μg/mL) and TNFα (50 ng/mL) for 36 to 48 hours. Some groups of cells were also exposed to (i) TNFα (50 ng/mL)/IL1β (25 ng/mL)/IL6 (1,000 U/mL)/PGE_2 (1 nmol/L), (ii) LPS (1 μg/mL)/IFNγ (1,000 U/mL), or (iii) TNFα (50 ng/mL)/IL1β (25 ng/mL)/pI:C (20 μg/mL)/IFNα (3,000 U/mL)/IFNγ (1,000 U/mL; ref. 19). For phenotyping, immature DCs were exposed to LPS/TNFα for 3 to 6 hours prior to drug treatment for 24 to 36 hours. Drug-induced changes are indicated by $\log_2$-fold changes of median fluorescence intensity (MFI) between drug- and DMSO-treated groups. The effects of drug interactions were determined by comparing the drug-induced changes of MFI between sum of monodrug treatments ($\Delta a+\Delta b$) and polydrug treatment (Δab), noninteraction ($\Delta a\approx 0$, or $\Delta b\approx 0$), additive interaction ($\Delta a+\Delta b\approx\Delta ab$, and $\Delta a^{*}\Delta b>0$), synergistic interaction ($|\Delta a+\Delta b|<|\Delta ab|$, and $\Delta a^{*}\Delta b>0$), and antagonistic interaction ($|\Delta a+\Delta b|>|\Delta ab|$, or $\Delta a^{*}\Delta b<0$). The ICT107 cancer vaccine consists of purified mature DCs pulsed with peptides representing tumor antigens and were provided by ImmunoCellular Therapeutics, Ltd. The preparation of ICT107 vaccine used in a phase I trial was described previously (20). Briefly, adherent cells from leukapheresis products were cultured for 5 days in RPMI1640 with 10% autologous serum supplemented with recombinant human GM-CSF (Berlex, 800 U/mL) and IL4 (R&D Systems, 500 U/mL) and matured by TNFα (R&D Systems, 50 ng/mL) for 3 to 4 days. Peptides included HLA-A1 restricted, MAGE$1_{(161\text{-}191)}$ [EADPTGHSY], AIM-2 [RSDSGQQARY], and HLA-A2 restricted, GP$100_{(209\text{-}217)}$ [IMDQVPFSV], TRP$2_{(180\text{-}188)}$ [SVYDFFVWL], HER$2_{(773\text{-}782)}$ [VMAGVGSPYV], and IL13Rα$2_{(345\text{-}354)}$ [WLPFGFILI] (Clinalfa). Cells from day 8 to 9 cultures were cultured at 10^6/mL with peptides (10 μg/mL per antigen) for 16 to 20 hours.

In vitro moDC function assay

T cells from healthy HLA-$A2^{+}$ donors were engineered with DMF5 T-cell receptor (TCR) or NY-ESO-1 TCR. Cells were labeled with eFluor 450 proliferation dye (65-0842-85, Thermo Fisher Scientific) according to the manufacturer's standard protocol. DMSO- or drug-treated autologous moDCs were loaded with 10 μg/mL of MART$1_{27\text{-}35}$ or NY-ESO-$1_{157–165}$ peptide and mixed with eFluor 450–labeled, cognate TCR-engineered T cells at DC:T-cell ratio of 1:320 to 1:40. T cells were cultured in the presence of IL2 at 10 U/mL. Antigen-pulsed, DMSO- or drug-treated ICT107 DCs were cultured with autologous lymphocytes at DC:T-cell ratio of 1:40 or 1:10. Four days later, cells were stained with anti-CD8α and MART1 tetramer/NY-ESO-1 pentamer/HLA-A2:Ig dimer and analyzed by flow cytometry.

Xenogeneic murine tumor model

Studies were approved by the University of Maryland, Baltimore (UMB) Institutional Animal Care and Use Committee.

Four- to 8-week-old male NOD.Cg-*Prkdc*^{scid} *Il2rg*^{tm1Wjl}/SzJ (NSG) mice were purchased from veterinary resources of UMB. NSG mice were injected with U87 GBM cells subcutaneously (s.c.) on the right flank (3×10^6 cells per injection). U87 GBM cells were cultured for 10 to 14 days before injection into mice and were authenticated within a year of their use. All cultures were *Mycoplasma* negative.

ICT107 vaccines were treated by DMSO or drugs for 24 to 36 hours and pulsed by peptide GP100$_{(209\text{-}217)}$, TRP2$_{(180\text{-}188)}$, HER2$_{(773\text{–}782)}$, and IL13Rα2$_{(345\text{-}354)}$ (10 μg/mL for each). On days 14 and 21, tumor-bearing mice were intravenously (i.v.) injected with either patient-derived T cells alone (1×10^7 cells/injection) or T cells plus ICT107 vaccine (2×10^6 cells per injection). Human IL2 was administered intraperitoneally (i.p.) daily for 3 days (10,000 IU/mouse/injection) following T-cell transfer. Mouse body weight and tumor sizes were measured every 3 days. Tumor volume was calculated by the modified ellipsoid formula (21): Tumor volume = 1/2(length × width^2). Mice were euthanized on day 37, and tumor-reactive T cells isolated from blood, spleen, and tumor were quantified and analyzed using anti-CD8α, anti-CD3, and HLA-A2:Ig dimers.

Statistical analysis

Results of ELISA and flow cytometry analysis were normalized to control if needed and analyzed by *t* test. Results of HLA-A2:Ig dimer staining were normalized by subtracting the results of solvent-loaded HLA-A2:Ig dimer. Animal studies contained 5 to 6 animals per group for tumor growth and 3 to 6 per group for *ex vivo* flow cytometry analysis. Tumor growth was analyzed by two-way ANOVA with Bonferroni posttests for all groups. The values and error bars represent mean ± SEM (*, $P \leq 0.05$; **, $P \leq 0.01$; ***, $P \leq 0.001$).

Results

Kinase inhibitors that influence moDC immunogenic phenotype

Sixty kinase inhibitors, listed in Supplementary Table S1, were selected on the basis of their FDA approval as anticancer agents or because of their ability to modulate the expression of MHC class I, MHC class II, and immunosuppressive proteins including PD-L1, CD155, and CD73 on melanoma cell lines (22). We first evaluated drug toxicity on moDCs following exposure to different concentrations of kinase inhibitors. Most compounds had little effect on cell viability at 0.3 μmol/L, and less than 6% of drugs reduced cell viability at 3 μmol/L (Fig. 1A). At 10 μmol/L, however, nearly 20% of drugs, most of which targeted the EGFR, PDGFR, and/or the PI3K/AKT signaling pathways, induced moDC cell death (Fig. 1A).

Next, we evaluated the effects that kinase inhibitors had on expression of cell surface proteins on moDCs that activate T cells. We also assessed CCR7 expression on moDCs as this receptor plays a role in their survival and migration to lymph nodes (23). Changes in the MFI of MHC class I, MHC class II, CD83, PD-L1, PD-L2, and CCR7 were plotted in 3D charts to visualize the impact that each drug had on expression of the indicated cell surface molecules. The data in Fig. 1B highlight the 10 drugs that most impacted expression of these surface molecules on moDCs. At 0.3 μmol/L, 3 MEK inhibitors, trametinib, AS703026, and selumetinib, respectively, induced the most substantial increases in CD83 and MHC class I. Increasing drug concentrations to 3 μmol/L further increased their expression. Although MEK inhibitors increased PD-L1 and PD-L2 expression at 3 μmol/L, DNA-PK inhibitor NU7441 downregulated PD-L1 and PD-L2 and simultaneously increased MHC class I (Fig. 1B). PP-121, a multitargeted inhibitor of PDGFR, mTOR, and DNA-PK, also downregulated PD-L1 and PD-L2 expression and moderately upregulated CCR7 and MHC class I. Of the compounds tested, MK2206 was the most effective at augmenting CCR7 expression but also exhibited high toxicity at 3 μmol/L. MK2206 moderately reduced PD-L1 and PD-L2 expression (Fig. 1B). Lapatinib, an EGFR/HER2 inhibitor, increased CCR7 and reduced PD-L1, PD-L2, MHC class I, and MHC class II expression. Another EGFR/HER2 inhibitor, mubritinib, had similar effects as lapatinib except that it reduced MHC class II expression. The mTOR inhibitor everolimus increased MHC class II expression and reduced PD-L1, CCR7, and MHC class I expression. The PLK1 inhibitor volasertib decreased PD-L1, PD-L2, MHC class I, and CD83 expression. Despite targeting similar enzymes, other inhibitors targeting PDGFR, mTOR, and PI3K did not mimic the effects of PP-121. MK2206, NU7441, trametinib, AS703026, PP-121, and selumetinib were identified as the most effective compounds that modulated expression of numerous cell surface proteins favoring T-cell activation. The effects of the top 6 drugs were validated using freshly prepared compounds (Fig. 1C). We observed that MK2206 was most efficient at increasing CCR7 (4.37±1.12-fold over DMSO control–treated cells, $P < 0.05$). MK2206 moderately reduced PD-L1 (0.68 ± 0.07-fold, $P < 0.05$) and PD-L2 (0.73 ± 0.03-fold, $P < 0.001$) expression. NU7441 increased MHC class I expression (1.4 ± 0.05-fold, $P < 0.001$) and reduced PD-L1 (0.44 ± 0.02-fold, $P < 0.001$) and PD-L2 expression (0.55 ± 0.09-fold, $P < 0.05$). Trametinib and selumetinib were both effective at increasing MHC class I (1.76 ± 0.09-fold, $P < 0.001$ and 1.49 ± 0.17-fold, P <0.05, respectively) but also at increasing PD-L1 (1.51 ± 0.18-fold, $P < 0.05$ and 1.24 ± 0.08, $P < 0.05$) and PD-L2 (1.67 ± 0.14-fold, $P < 0.05$ and 1.52 ± 0.22, $P = 0.07$) expression.

Beneficial interactions in combining MK2206, NU7441, and trametinib

We investigated the effect that combining MK2206, NU7441, and trametinib had on the expression of various T-cell–stimulatory cell surface proteins on moDCs. We first optimized drug concentrations to reduce toxicity (Fig. 2A, left). At 20 nmol/L, MK2206 could not significantly increased CCR7 but still slightly decreased PD-L1 and PD-L2 expression by 10% ($P < 0.05$; Fig. 2A, right). At 2 μmol/L, NU7441 maintained its ability to increase MHC class I and reduce PD-L1 and PD-L2. At 20 nmol/L, trametinib increased MHC class I, CCR7, and CD83 but also increased PD-L1. Combining MK2206 and NU7441 (referred to as MKNU) increased MHC class I expression to a greater extent than either of these drugs alone. Furthermore, PD-L1 and PD-L2 expression was decreased but to no greater extent than NU7441 alone. Combining NU7441 and trametinib (NUTRA) was also more effective at augmenting MHC class I and CCR7 expression as compared with monodrug treatment. This combination also decreased PD-L2 more effectively than did single-drug treatment. Although NU7441 did not impact CCR7 expression at 2 μmol/L, it exhibited synergistic effects when combined with trametinib. MK2206 plus trametinib (MKTRA) upregulated MHC class I and CD83 expression, whereas NU7441 plus trametinib upregulated MHC class I but reduced CD83 expression. Combining

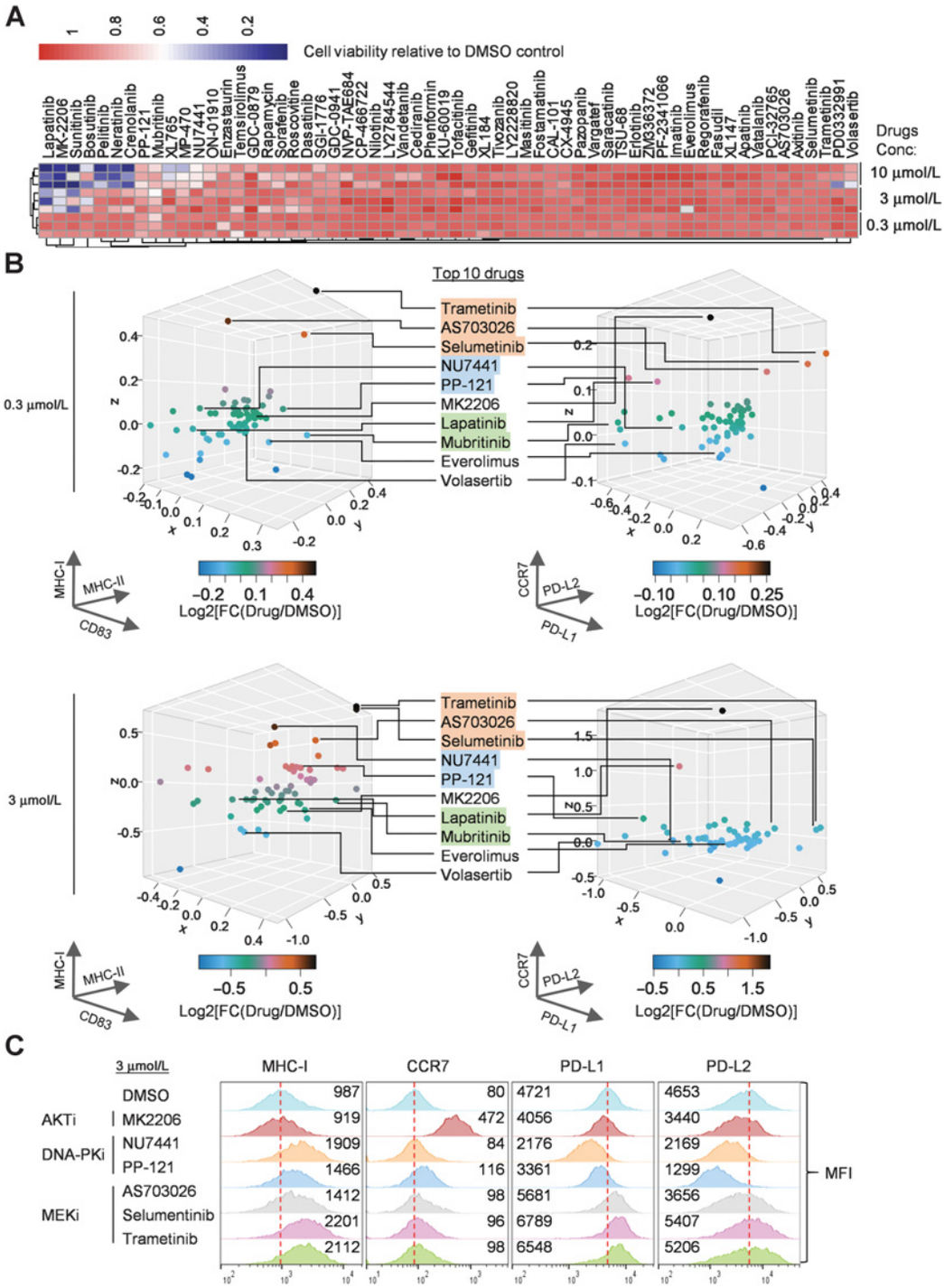

Figure 1.

Screening a kinase inhibitor library for positive modulators of moDC immunogenic phenotype. **A,** Human primary moDCs were cultured in the presence of 300 nmol/L, 3 μmol/L, and 10 μmol/L of the indicated drugs for 24 to 36 hours during the DC maturation process. Cell death (relative to DMSO control) was plotted by the pheatmap package in R. Data represent means of three independent experiments. Conc., concentration. **B,** moDCs were treated with the indicated drugs at 0.3 μmol/L and 3 μmol/L during the maturation process. Relative expression of MHC class I, MHC class II, CD83, CCR7, PD-L1, and PD-L2 was determined by flow cytometry (MFI fold change of drug-treated group to DMSO control) from three independent experiments and plotted in 3D scatter charts generated by R package scatter3D. 3D images were generated using the top 10 lead drugs. Drugs that target the same pathways are highlighted in similar colors. Data represent means of three independent experiments. **C,** moDCs were treated with MK2206, NU7441, PP-121, AS702036, selumetinib, and trametinib (3 μmol/L) during DC maturation. MFI values are indicated next to each histogram. Red dashed line represents the MFI of the control group.

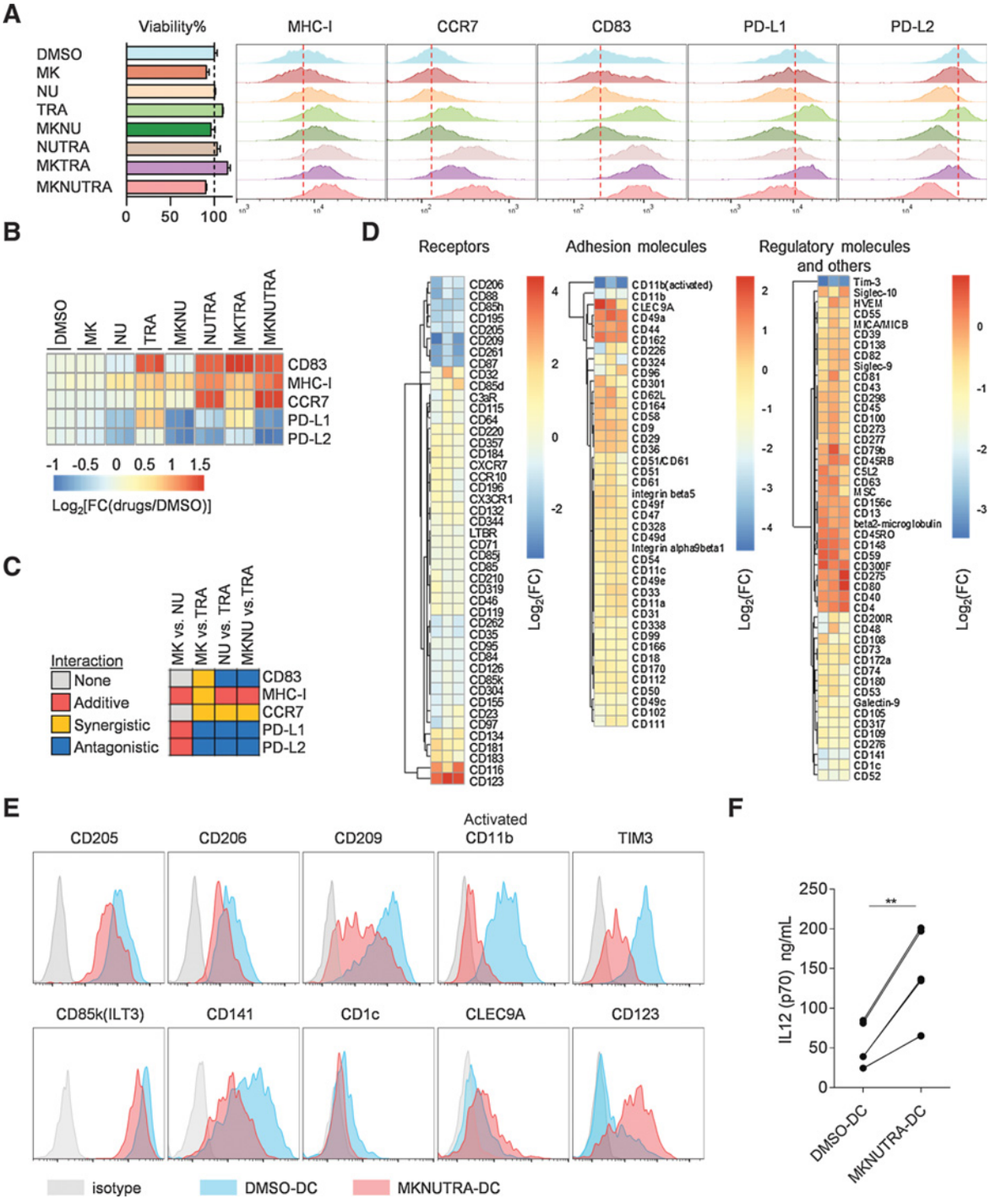

Figure 2.

Effects of low-dose MK2206, NU7441, and trametinib on moDC immunogenic phenotype in single-, dual-, and triple-drug use. **A,** MK2206 (MK, 20 nmol/L), NU7441 (NU, 2 μmol/L), and trametinib (TRA, 20 nmol/L) were added individually or in combination during the moDC maturation process. After 24 to 36 hours, cell viability and expression of MHC class I, CCR7, CD83, PD-L1, and PD-L2 were determined by flow cytometry. The red dashed line represents MFI of DMSO-treated cells. **B,** Heatmaps represent fold changes in MFI relative to DMSO-treated cells, and interactions among drugs were calculated on the basis of MFI changes and are indicated in **C**. **D,** The expression of 335 surface molecules on control DMSO- and MKNUTRA-treated moDCs was analyzed by flow cytometry. Heatmaps represent the MFI fold changes relative to DMSO-treated cells. **E,** Representative histograms demonstrating changes in the expression levels of key surface molecules altered by MKNUTRA treatment. Isotype (light gray), DMSO (light blue), and MKNUTRA (light red). **F,** IL12p70 produced by moDCs from several donors was measured by ELISA 24 to 36 hours after treatment with DMSO or MKNUTRA. All data represent at least three independent experiments (**, $P < 0.05$, paired t test).

all 3 drugs (MKNUTRA) increased MHC class I, CCR7, and CD83, and decreased PD-L1 to a greater extent than did mono- or dual-drug treatment (Fig. 2A and B). The data in Fig. 2C highlight the additive, synergistic, or antagonistic impact that combination therapies had on expression of activation proteins on moDCs.

To further understand how MKNUTRA treatment impacted cell membrane proteins of moDCs, we evaluated expression of 335 surface markers by flow cytometry. Cell surface proteins were categorized as receptors, adhesion molecules, or regulator molecules (Fig. 2D). Among receptors, MKNUTRA most decreased expression of CD205, CD206, and CD209. These changes are reflective of more mature moDCs. Several molecules associated with negative immunoregulation were also downregulated in response to MKNUTRA, including CD85k (ILT3). Of adhesion molecules, CD11b was the most downregulated in response to treatment. MKNUTRA also downregulated Tim-3 (Fig. 2D, regulatory molecules). The DC subset lineage markers CD123 and

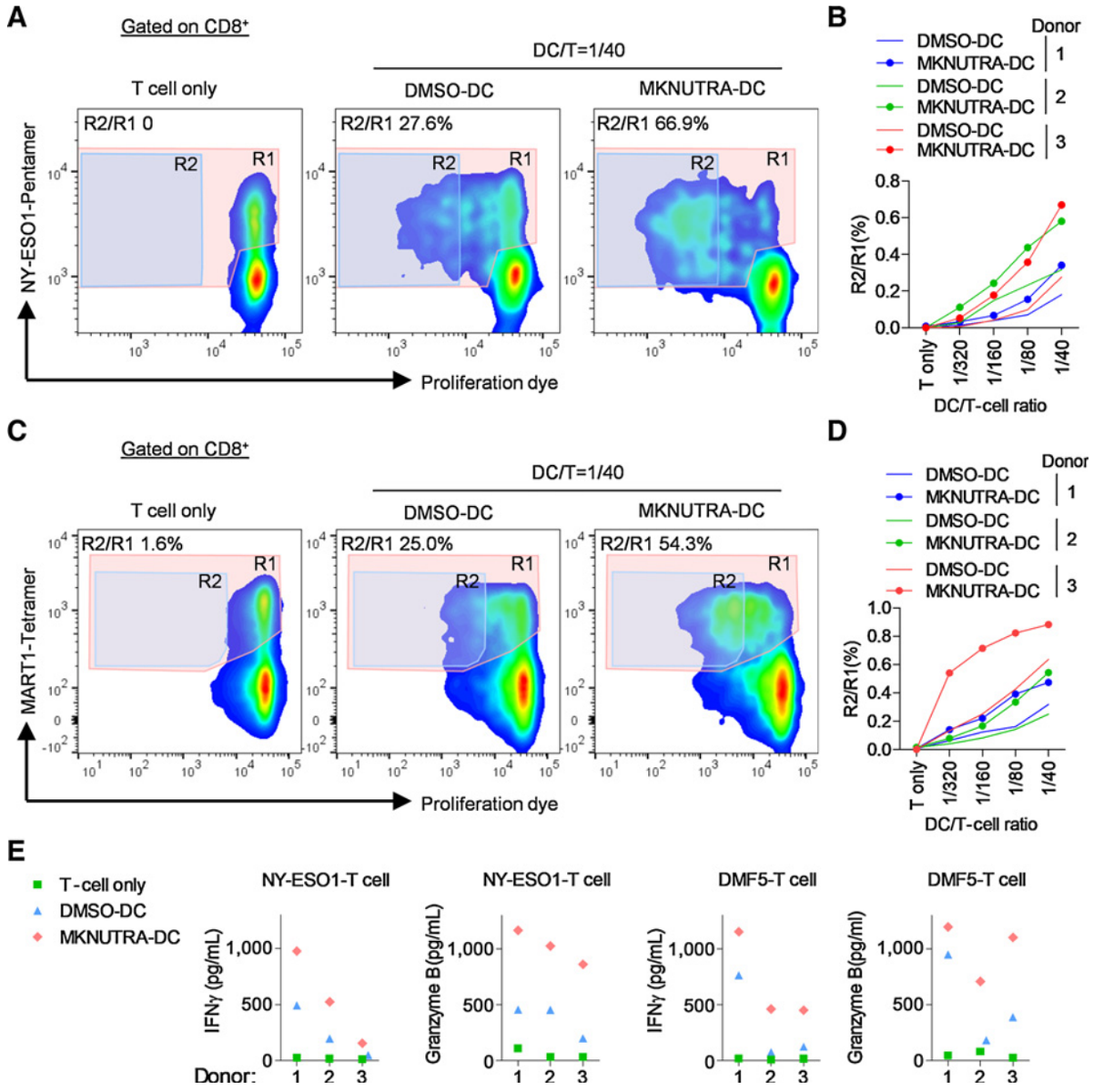

Figure 3.

MKNUTRA augments moDC function to stimulate TCR-engineered T cells. $CD8^+$ T cells engineered to express the NY-ESO-1 TCR (**A**) or DMF5 TCR (**C**) were labeled with eFluor 450 proliferation dye and stimulated with autologous DMSO- or MKNUTRA-treated moDCs pulsed with peptides representing the NY-ESO-$1_{(157\text{-}165)}$ or $MART1_{(27\text{-}35)}$ antigens. TCR-engineered autologous T cells were cultured at DC:T-cell ratio of 1:320 to 1:40. Four days later, cells were stained by NY-ESO-$1_{(157\text{-}165)}$ pentamer or $MART1_{(27\text{-}35)}$ tetramer and anti-CD8α and analyzed by flow cytometry. R2/R1 values are indicated in **A** and **C**. **B** and **D** show the extent of T-cell proliferation at different DC:T-cell ratios. **E,** IFNγ and granzyme B production by NY-ESO-1 TCR– or DMF5 TCR–engineered T cells in response to stimulation with DMSO- or MKNUTRA-treated moDCs at a DC:T-cell ratio of 1:80. All data represent at least three independent experiments.

CLEC9A were also upregulated, whereas CD141 and CD1c expression was reduced following treatment (Fig. 2D). Histograms demonstrating such changes following MKNUTRA treatment are shown in Fig. 2E. In addition to induction of phenotypic changes, drug exposure altered DC function, as demonstrated by increased IL12p70 production (Fig. 2F).

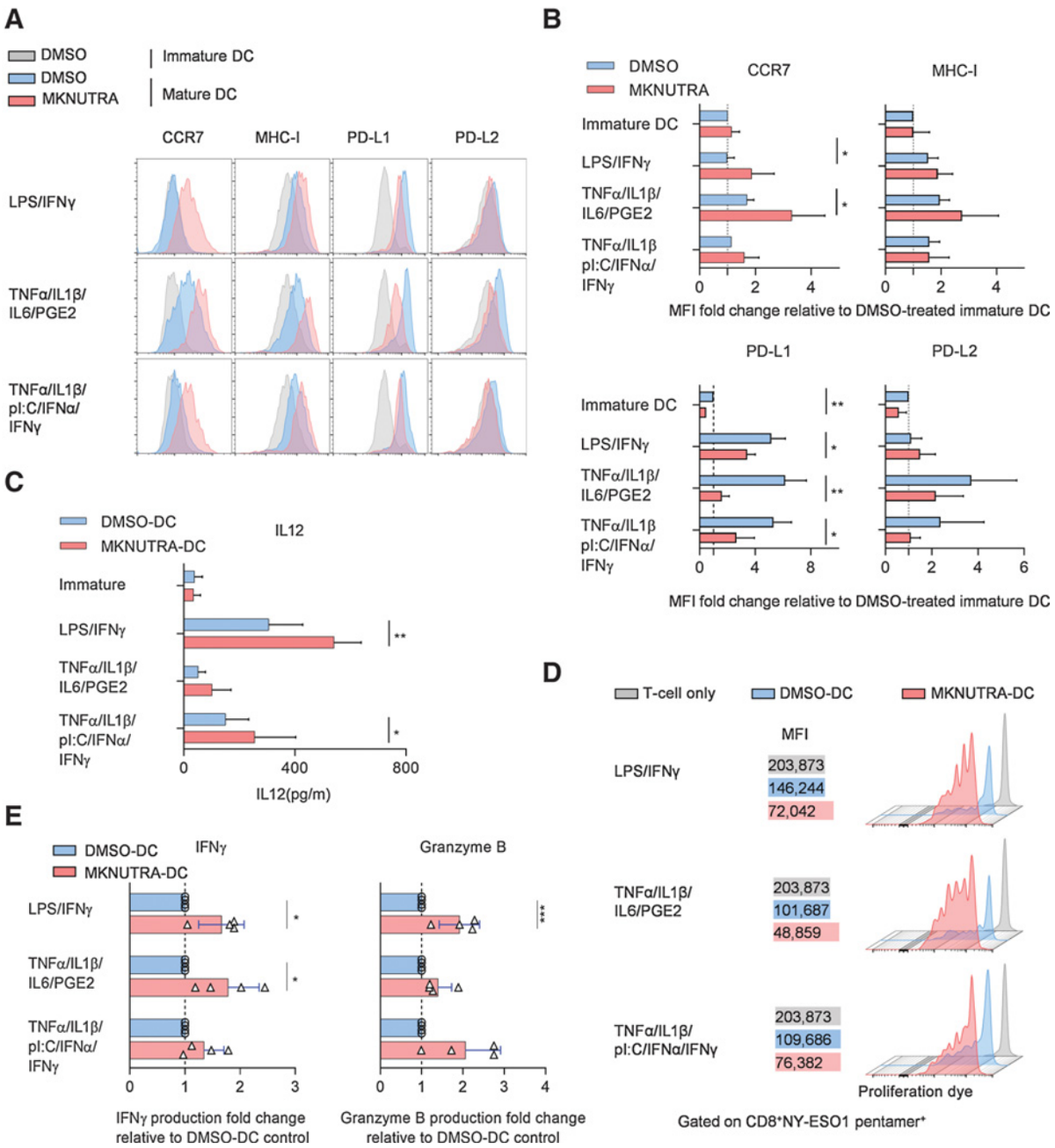

Figure 4.

MKNUTRA enhances the effects of other moDC maturation cocktails. **A,** moDCs were matured with LPS/IFNγ, TNFα/IL1β/IL6/PGE_2, or TNFα/IL1β/pI:C/IFNα/IFNγ in the presence of either DMSO (light blue) or MKNUTRA (light red), and expression of CCR7, MHC class I, PD-L1 and PD-L2 was measured by flow cytometry. **B,** Fold changes in MFI relative to DMSO-treated immature moDCs. Cells were gated on live and $CD209^+$ cells. **C,** IL12p70 production by moDCs matured using the conditions shown in **A** were determined by ELISA. **D,** moDCs were matured using the conditions described in **A** and then pulsed with the NY-ESO-$1_{(157\text{-}165)}$ peptide. eFluor 450–labeled NY-ESO-1 TCR–engineered T cells were cultured with indicated moDCs for 4 days, at which time NY-ESO-1 TCR proliferation was determined on the basis of eFluor 450 dilution. T cells were gated on CD8α and NY-ESO-$1_{(157\text{-}165)}$ pentamer, and eFluor 450 MFI is shown to the left of histograms. **E,** IFNγ and granzyme B production after 2 days of coculturing NY-ESO-1 TCR–engineered T cells with indicated moDCs at a DC:T-cell ratio of 1:80 was determined by ELISA. All data represent at least three independent experiments. Each symbol represents one donor (*, $P < 0.05$; **, $P < 0.01$; ***, $P < 0.001$).

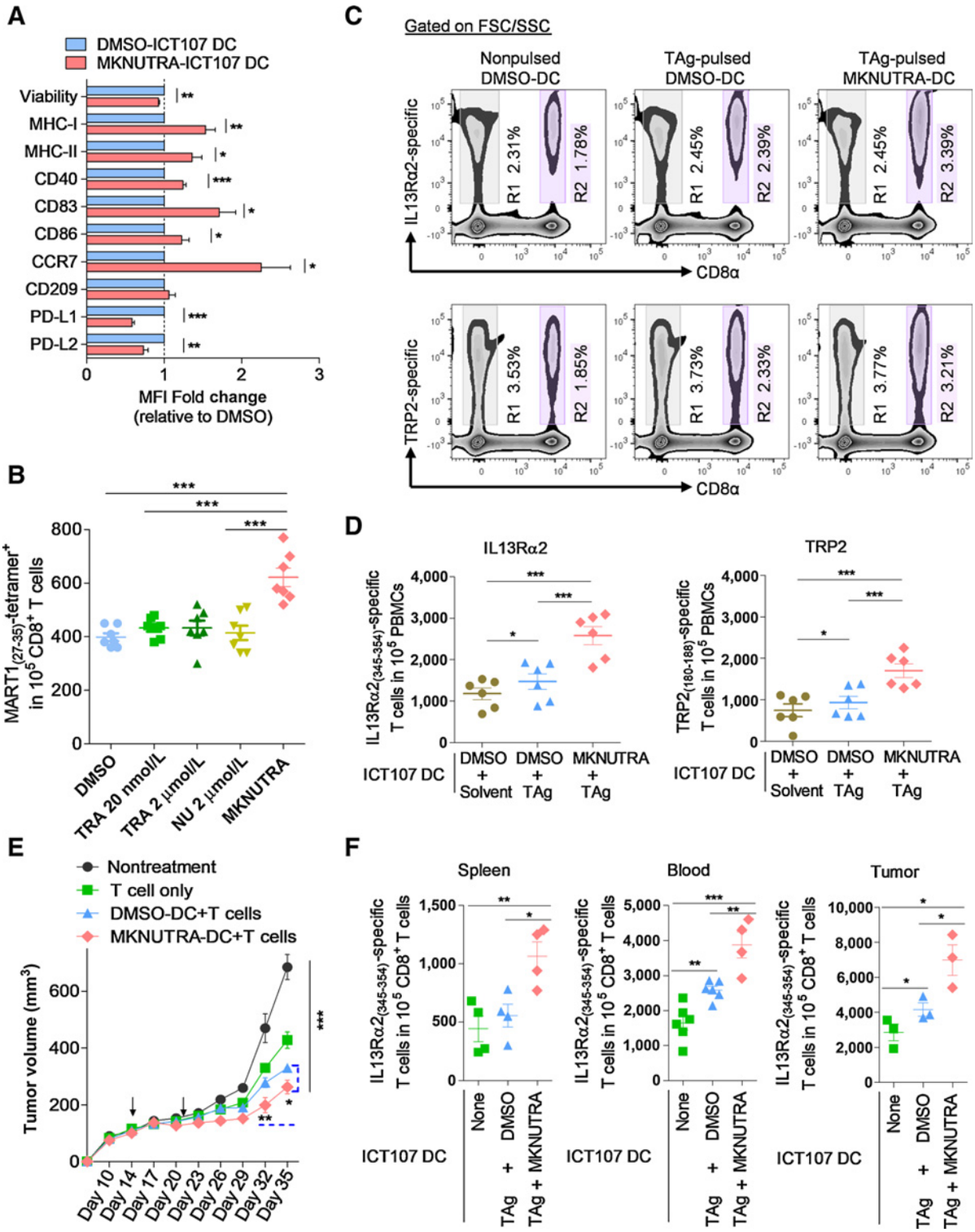

Figure 5.

MKNUTRA improves ICT107 cancer vaccine *in vitro* and in xenogeneic murine tumor model. **A,** ICT107 DCs were treated by DMSO or MKNUTRA for 24 hours. Cells were gated on live and CD209$^+$ cells for analysis. Changes in viability and the MFI of the indicated proteins between MKNUTRA-treated ICT107 (MKNUTRA-ICT107 DC, light red bar) and DMSO-treated ICT107 (DMSO-ICT107 DC, light blue bar) are shown. **B,** ICT107 DCs were treated with vehicle control DMSO (•), 20 nmol/L trametinib (TRA, ■), 2 μmol/L TRA (▲), 2 μmol/L NU7441 (NU, ▼), or MKNUTRA (◇) for 24 hours. (*Continued on the following page.*)

Taken together, these data show that low-dose combination treatment with MK2206, NU7441, and trametinib induces phenotypic and functional changes that favor their ability to activate T cells.

MKNUTRA augments moDC ability to stimulate tumor-reactive T cells *in vitro*

To determine the effect that MKNUTRA treatment had on moDC ability to stimulate T cells of a known tumor antigen specificity, we engineered T cells to express a TCR specific for the NY-ESO-$1_{(157\text{-}165)}$ peptide and stimulated them with autologous moDCs pulsed with the NY-ESO-$1_{(157\text{-}165)}$ peptide. In the absence of moDCs, $CD8^+$ NY-ESO-1 pentamer$^+$ T cells did not proliferate (Fig. 3A). However, 27.6% of $CD8^+$ NY-ESO-1 pentamer$^+$ T cells activated with DMSO-treated moDCs underwent at least two cell divisions. In contrast, more than double the amount of $CD8^+$ NY-ESO-1 pentamer$^+$ T cells (66.9%) stimulated with MKNUTRA-treated moDCs underwent multiple rounds of cell division. We also investigated T-cell proliferation in response to activation with varying numbers of DCs from various donors and found that MKNUTRA treatment augmented moDC stimulatory capacity (Fig. 3B). Likewise, MKNUTRA-treated moDCs demonstrated enhanced ability to activate T cells engineered to express the TCR reactive toward Melan-A/MART$1_{(27\text{-}35)}$ (DMF5; Fig. 3C and D). Enhanced proliferation was mirrored by the increased propensity of T cells to produce IFNγ and granzyme B when stimulated with MKNUTRA-treated moDCs (Fig. 3E).

MKNUTRA enhances effects of other moDC maturation protocols

We next investigated whether MKNUTRA improved the maturation status and function of other stimuli typically used to generate and activate moDCs. Three different clinical-grade maturation cocktails were tested: Cocktail "A" consisted of TNFα/IL1β/IL6/PGE_2 (24), cocktail "B" of LPS/IFNγ (25), and cocktail "C" of TNFα/IL1β/pI:C/IFNα/IFNγ (19). Cocktails B and C both produced IL12. Expression of CCR7, MHC class I, PD-L1, and PD-L2 was compared between immature moDCs and moDCs activated with each of the cocktails with or without MKNUTRA. We found that only cocktail A induced higher expression of CCR7, MHC class I, PD-L1, and PD-L2 relative to moDCs treated with LPS/IFNγ or with TNFα/IL1β/IL6/PGE_2 (Fig. 4A). Adding MKNUTRA to cocktails A, B, or C further increased CCR7 and MHC class I production and reduced PD-L1 and PD-L2 expression. Figure 4B summarizes data collected from several donors and demonstrates fold changes (over immature DCs) in the expression of the indicated molecules. Although treatment with cocktail B or C increased IL12 production over cells treated with cocktail A, MKNUTRA augmented IL12 production (Fig. 4C).

We investigated the impact that MKNUTRA had on moDC ability to stimulate tumor antigen–reactive T cells in the context of these different maturation cocktails. For these studies, moDCs were matured with the various cocktails indicated in Fig. 4D and in the presence of MKNUTRA or DMSO control. moDCs were pulsed with NY-ESO-$1_{(157\text{-}165)}$ peptide, and their ability to activate autologous T cells engineered to express NY-ESO-1 TCR was assessed by measuring IFNγ or granzyme B production. We observed that at the 1:80 of DC:T-cell ratio used, MKNUTRA increased moDC ability to induce NY-ESO-1 T-cell proliferation regardless of how moDCs were matured (Fig. 4D). Likewise, MKNUTRA treatment augmented production of IFNγ and granzyme B (Fig. 4E).

MKNUTRA improves ICT107 function and T-cell activity from patients with GBM

We next investigated the effects that MKNUTRA had on ICT107 viability and phenotype. ICT107 is an moDC-based cancer vaccine that has completed both phase I (20) and phase II (NCT01280552) clinical trials for patients with newly diagnosed GBM. Briefly, ICT107 cells were prepared from leukapheresis products of patients with GBM by treating adherent cells with GM-CSF/4 for differentiation; TNFα was used to mature DCs (20). As shown in Fig. 5A, MKNUTRA reduced DC viability less than 8%. However, MKNUTRA treatment increased MHC class I, MHC class II, CD40, CD83, CD86, and CCR7 expression and concurrently decreased PD-L1 and PD-L2 expression (Fig. 5A). In addition, MKNUTRA-treated ICT107 demonstrated an enhanced ability to augment MART-1–reactive T-cell numbers as compared with T cells activated with DMSO- or single-drug–treated ICT107 (Fig. 5B).

ICT107 was designed as a six peptide–pulsed DC vaccine, of which four peptides, GP$100_{(209\text{-}217)}$, TRP$2_{(180\text{-}188)}$, HER$2_{(773\text{-}782)}$, and IL13Rα$2_{(345\text{-}354)}$, are presented by HLA-A2. We sought to determine the impact that MKNUTRA-treated ICT107 had on expansion of naturally occurring tumor antigen–reactive T cells from patients with GBM. Autologous PBMCs were cocultured with MKNUTRA-treated ICT107 loaded with TRP$2_{(180\text{-}188)}$ and IL13Rα$2_{(345\text{-}354)}$ peptide. The frequency of antigen-reactive T cells was determined by flow cytometry after 4 days (Fig. 5C). Antigen-specific $CD8^+$ T cells were quantified using peptide-loaded HLA-A2:Ig dimer. We observed that patients had a preexisting population of circulating antigen-reactive T cells and that these frequencies varied between patients (Supplementary Fig. S1). However, T cells reactive toward these peptides were not detectable in healthy donors. Exposure of autologous T cells to DMSO-treated ICT107 increased the frequencies of IL13Rα$2_{(345\text{-}354)}$– and TRP$2_{(180\text{-}188)}$–specific $CD8^+$ T cells by approximately 25% ($P < 0.05$; Fig. 5C and D). In contrast, MKNUTRA-treated

(*Continued.*) After this time, ICT107 DCs were cultured with autologous GBM patient-derived PBMCs at a DC:T-cell ratio of 1:40 for 4 days. The frequencies of tumor-reactive T cells were determined by gating on CD8α and MART$1_{(27\text{-}35)}$ tetramer cells. **C** and **D,** ICT107 DCs were treated with DMSO or MKNUTRA for 24 hours. After this time, cells were washed and then cocultured for 4 days with autologous PBMCs derived from GBM patients at a DC:T-cell ratio of 1:10. The numbers of IL13Rα$2_{(345\text{-}354)}$– and TRP$2_{(180\text{-}188)}$–specific $CD8^+$ T cells were determined by flow cytometry using HLA-A2-peptide:Ig dimers. In **D**, each symbol represents a different patient. Results of HLA-A2:Ig dimer staining were normalized by subtracting the results of non-peptide–pulsed HLA-A2:Ig dimer control. **E,** Mice ($n = 5$–6/group) were injected subcutaneously with U87 GBM cells. Fourteen and 21 days after tumor cell injection, mice received MKNUTRA- or DMSO-treated ICT107 DCs and GBM patient–derived T cells (enriched from PBMCs). Alternatively, mice remained untreated or received T cells only. Statistical differences were determined by two-way ANOVA with Bonferroni posttests for all groups (vertical black bar) and detailed comparisons between DMSO-DC and MKNUTRA-DC treatment (blue dashed bar, days 32–35). **F,** The abundance of IL13Rα$2_{(345\text{-}354)}$–specific $CD8^+$ T cells in the spleen, peripheral blood, and tumor of tumor-bearing mice was determined using IL13Rα$2_{(345\text{-}354)}$–loaded HLA-A2:Ig dimer, as described in **D**. The data shown in **A, B, D,** and **F** represent at least three independent experiments and show the mean ± SEM (*, $P < 0.05$; **, $P < 0.01$; ***, $P < 0.001$ analyzed by *t* test).

ICT107 increased the number of these cells by more than 1-fold ($P < 0.001$). The percentage of $GP100_{(209\text{-}217)}$– and $HER2_{(773\text{-}782)}$–specific $CD8^+$ T cells was generally below 1%, and their frequency was not altered following exposure to DMSO- or MKNUTRA-treated ICT107 (Supplementary Fig. S2).

We investigated the antitumor efficacy of MKNUTRA-treated ICT107 plus autologous T cells in mice bearing an established GBM tumor. NSG mice were implanted with human HLA-$A2^+$ U87 GBM cells, which express GP100, HER2, and IL13Rα2, but not TRP2 (26). Tumor-bearing mice were injected with HLA-$A2^+$ patient-derived peripheral T cells with or without autologous DMSO- or MKNUTRA-treated ICT107. As shown in Fig. 5E, mice injected with T cells alone exhibited delayed tumor growth and were comparable with untreated mice. These data suggest that the preexisting population of GBM-reactive T cells mediated a small degree of immunity. Mice injected with DMSO-treated ICT107 plus T cells exhibited slower tumor growth as compared with mice injected with T cells alone, highlighting the DCs ability to enhance T-cell activity in tumor-bearing mice. At later time points, mice treated with MKNUTRA-treated ICT107 and T cells demonstrated greater antitumor activity than mice treated with DMSO-treated ICT107. We also analyzed frequencies of the tumor antigen–specific T cells *ex vivo* in the blood, spleen, and tumor. Only $IL13R\alpha2_{(345\text{-}354)}$ peptide–specific T cells were detected by HLA-A2-peptide:Ig dimer staining. The number of $GP100_{(209\text{-}217)}$–, $HER2_{(773\text{-}782)}$–, and $TRP2_{(180\text{-}188)}$–specific T cells were below the threshold of detection. The frequency of $IL13R\alpha2_{(345\text{-}354)}$ peptide–specific T cells in mice treated with MKNUTRA-treated ICT107 was higher than in mice treated with DMSO-treated ICT107 (Fig. 5F), supporting our *in vitro* data demonstrating improved T-cell activation by MKNUTRA-treated DCs.

Discussion

In this study, we identified compounds that augment DC immunogenicity resulting in enhanced T-cell activity toward tumor antigens. We screened kinase inhibitors for their ability to positively modulate moDC phenotype and capacity to activate tumor-reactive T cells. MK2206, NU7441, and trametinib were found to be effective at altering expression of several cell surface costimulatory and coinhibitory molecules as well as chemokine receptors on moDCs, improving moDC ability to activate T cells. Identifying strategies to ensure consistent generation of high-quality moDCs will maximize their potential to activate T cells and prevent immune exhaustion or tolerance (10).

We observed that MEK inhibitors such as trametinib enhanced moDC maturation, as reflected by their ability to increase MHC class I, MHC class II, and CCR7 expression. These findings are in agreement with previous reports demonstrating the propensity for ERK inhibitors to enhance TNF's or LPS's ability to activate DCs (27, 28). CCR7 directs mature DCs to secondary lymphoid tissues and enhances DC survival (27). Despite MEK inhibitors' ability to alter expression of these molecules, we found that MEK inhibitors (trametinib, AS703026, and selumetinib) upregulated expression of PD-L1 and PD-L2, which have the potential to restrict moDCs' ability to stimulate T cells. The DNA-PK inhibitor NU7441 also increased MHC class I expression but, in contrast to MEK inhibition, downregulated PD-L1 and PD-L2 surface expression and did not affect CCR7 expression. NU7441 reduced PD-L1 expression and increased MHC class I expression on melanoma cells (22). DNA-PK is involved in DNA double-strand break repair pathway (DSB) but can also impact transcriptional regulation by interacting with transcription factors (29). DSB can induce PD-L1 expression in cancer cells (30), in which DNA-PK may be involved. Here, were found that NU7441 downregulated PD-L1 and PD-L2 on moDCs. Although the precise mechanisms by which NU7441 impacts PD-L1 and PD-L2 expression on DCs is unknown, it is plausible that reactive oxygen species (ROS) generated by monocytes in response to GM-CSF (31) induces DNA damage and contributes to reduced PD-L1 expression in the presence of NU7441. GM-CSF– and IL4-induced moDC differentiation has also been shown to upregulate DNA-PK expression and may render moDCs resistant to ROS in the presence of NU7441 (32).

The combination of MK2206, NU7441, and MEK inhibitors generated moDCs with properties for activating T cells including elevated expression of CCR7, MHC, and CD83 and reduced expression of PD-L1 and PD-L2. Scrutinizing several hundred cell surface proteins on MKNUTRA-treated moDCs revealed that combination treatment decreased expression of CD206 and CD209. CD206 and CD209 are involved in antigen uptake and are typically expressed on mature moDCs (33–35). Our data indicate that MKNUTRA–treated moDCs seemed less likely to be tolerogenic based on the downregulation of several immunoinhibitory proteins including PD-L1, PD-L2, ILT3 (CD85k; refs. 36, 37), CD11b (38), and TIM3 (39). MKNUTRA also increases IL12 production, necessary for optimal T-cell activation (40). Tim-3 reduces DC antitumor potential by reducing their ability to respond to TLR-mediated activating signals, resulting in reduced production of type I IFNs and IL12 (41, 42). CD123 (aka 3RA) is a marker on plasmacytoid DCs and *in vitro* generated moDCs and defines a population of DCs with tumor-inhibiting activity. CLEC9A-expressing DCs have also been proposed as targets for *in vivo* vaccination due to their ability to produce inflammatory cytokines that drive T-cell activation (43, 44). Here, we found that both CD123 and CLEC9A expression on moDCs were increased upon MKNUTRA treatment. In addition, NF-κB functions in LPS-induced moDC maturation (45). In THP-1 cells, a human myelomonocytic cell line, NF-κB–dependent gene transcription was inhibited by constitutively active MEK1 via the inhibition of TATA-binding protein (TBP) phosphorylation (46). Previous studies also indicate that aryl hydrocarbon receptor (AhR) contributes to the MEK-dependent maintenance of an immature DC status (47). Therefore, it is conceivable that MEK inhibition during moDC maturation enhances the transcriptional activity and target occupancy of NF-κB and AhR, resulting in a more functional DC.

MKNUTRA-treated ICT107 demonstrated enhanced antitumor activity in mice with established GBM tumors. Increased activity was associated with increased tumor infiltration and 2- to 3-fold increases of $IL13R\alpha2_{(345\text{-}354)}$–reactive T-cell in peripheral tissues. MKNUTRA's ability to enhance moDC immunogenicity *in vivo* agrees with its propensity to induce development of an immunophenotypic profile that favors moDC longevity and T-cell activation. Despite MKNUTRA's ability to increase moDC immunogenicity, IL12 production, and T-cell activation *in vitro*, the enhanced anti-GBM activity was moderate and only observed at later time points. We speculate that antitumor efficacy was limited by the small numbers of tumor-reactive T cells as well as the dependence on a limited number of tumor antigen targets. For example, expression of tumor antigens IL13Rα2 and TRP-2 is greater than expression of GP100 (48) or HER-2 (49) in GBM

samples, as measured in a retrospective clinicopathologic study. That IL13Rα2 and TRP-2 are more prevalent was supported by our observations of higher frequencies of $IL13R\alpha2_{(345\text{-}354)}$– and $TRP2_{(180\text{-}188)}$–reactive $CD8^+$ T cells in GBM patient blood samples. $IL13R\alpha2_{(345\text{-}354)}$ peptide–pulsed DC vaccines demonstrate antitumor responses in a subset of HLA-A*24/A*02 patients with recurrent malignant glioma (50), which is consistent with the preferential expansion of $IL13R\alpha2_{(345\text{-}354)}$–reactive T cells in our study. Our tumor model used the $TRP2^-$ U87 GBM cell line, further limiting the number of tumor-reactive T cells that could respond. Thus, the suboptimal activation and frequencies of GP100 and HER-2–reactive T cells together with the lack of TRP-2 expression on U87 meant that the antitumor efficacy of DC-activated T cells relied entirely on $IL13R\alpha2_{(345\text{-}354)}$–reactive T cells to control tumor growth.

The inclusion of small-molecule inhibitors such as those described in these studies could offer additional opportunities to improve antitumor responses. In addition to improving the function of *in vitro*-prepared moDCs, these drugs also function as tumoricidal compounds *in vivo* and can modulate expression of immunosuppressive molecules (i.e., PD-L1, PD-L2, CD155, and others) and immunostimulatory and costimulatory molecules on cancer cell and tumor-infiltrating DCs (22).

Breakthroughs in cancer immunotherapies include the ability to target tumor-specific antigens such as neoantigens, T cells engineered to express tumor-reactive TCRs, use of tumor-infiltrating lymphocyte adoptive therapy (TIL) therapy, and immune checkpoint blockade. In each of these avenues, T-cell responses might be potentiated by incorporation of DCs.

Disclosure of Potential Conflicts of Interest.

S.J. Swanson is a Senior Vice President of Research at ImmunoCellular Therapeutics. No potential conflicts of interest were disclosed by the other authors.

Authors' Contributions

Conception and design: J. Guo, E. Davila
Development of methodology: J. Guo, E. Davila
Acquisition of data (provided animals, acquired and managed patients, provided facilities, etc.): J. Guo, A.J. Christians, S.J. Swanson
Analysis and interpretation of data (e.g., statistical analysis, biostatistics, computational analysis): J. Guo, E. Davila
Writing, review, and/or revision of the manuscript: J. Guo, A.J. Christians, S.J. Swanson, E. Davila
Administrative, technical, or material support (i.e., reporting or organizing data, constructing databases): J. Guo, E. Muse
Study supervision: E. Davila

Acknowledgments

This work was supported by R01CA207913, a research award from ImmunoCellular Therapeutics, VA Merit Award BX002142, University of Maryland School of Medicine Marlene and Stewart Greenebaum Comprehensive Cancer Center P30CA134274, and the University of Colorado Denver Comprehensive Cancer Center P30CA046934.

The costs of publication of this article were defrayed in part by the payment of page charges. This article must therefore be hereby marked *advertisement* in accordance with 18 U.S.C. Section 1734 solely to indicate this fact.

Received March 14, 2019; revised March 22, 2019; accepted June 28, 2019; published first July 2, 2019.

References

1. Butterfield LH. Dendritic cells in cancer immunotherapy clinical trials: are we making progress? Front Immunol 2013;4:454.
2. McIlroy D, Gregoire M. Optimizing dendritic cell-based anticancer immunotherapy: maturation state does have clinical impact. Cancer Immunol Immunother 2003;52:583–91.
3. Versteven M, Van den Bergh JMJ, Marcq E, Smits ELJ, Van Tendeloo VFI, Hobo W, et al. Dendritic cells and programmed death-1 blockade: a joint venture to combat cancer. Front Immunol 2018;9:394.
4. Holla S, Sharma M, Vani J, Kaveri SV, Balaji KN, Bayry J. GM-CSF along with IL-4 but not alone is indispensable for the differentiation of human dendritic cells from monocytes. J Allergy Clin Immunol 2014; 133:1500–2.
5. Sabado RL, Balan S, Bhardwaj N. Dendritic cell-based immunotherapy. Cell Res 2017;27:74–95.
6. Harman AN, Bye CR, Nasr N, Sandgren KJ, Kim M, Mercier SK, et al. Identification of lineage relationships and novel markers of blood and skin human dendritic cells. J Immunol 2013;190:66–79.
7. Collin M, Bigley V. Human dendritic cell subsets: an update. Immunology 2018;154:3–20.
8. Randolph GJ, Sanchez-Schmitz G, Liebman RM, Schakel K. The CD16(+) (FcgammaRIII(+)) subset of human monocytes preferentially becomes migratory dendritic cells in a model tissue setting. J Exp Med 2002;196: 517–27.
9. Sanchez-Torres C, Garcia-Romo GS, Cornejo-Cortes MA, Rivas-Carvalho A, Sanchez-Schmitz G. CD16+ and CD16- human blood monocyte subsets differentiate in vitro to dendritic cells with different abilities to stimulate CD4+ T cells. Int Immunol 2001;13:1571–81.
10. Dudek AM, Martin S, Garg AD, Agostinis P. Immature, semi-mature, and fully mature dendritic cells: toward a DC-cancer cells interface that augments anticancer immunity. Front Immunol 2013;4:438.
11. Castiello L, Sabatino M, Jin P, Clayberger C, Marincola FM, Krensky AM, et al. Monocyte-derived DC maturation strategies and related pathways: a transcriptional view. Cancer Immunol Immunother 2011;60:457–66.
12. Attie AD, Raines RT. Analysis of Receptor-Ligand Interactions. J Chem Educ 1995;72:119–24.
13. Abraham RS, Mitchell DA. Gene-modified dendritic cell vaccines for cancer. Cytotherapy 2016;18:1446–55.
14. Schenk PW, Snaar-Jagalska BE. Signal perception and transduction: the role of protein kinases. Biochim Biophys Acta 1999;1449:1–24.
15. Bhullar KS, Lagaron NO, McGowan EM, Parmar I, Jha A, Hubbard BP, et al. Kinase-targeted cancer therapies: progress, challenges and future directions. Mol Cancer 2018;17:48.
16. Klaeger S, Heinzlmeir S, Wilhelm M, Polzer H, Vick B, Koenig PA, et al. The target landscape of clinical kinase drugs. Science 2017;358. pii: eaan4368.
17. Wen PY, Reardon DA, Phuphanich S, Aiken R, Landolfi JC, Curry WT, et al. A randomized, double-blind, placebo-controlled phase 2 trial of dendritic cell (DC) vaccination with ICT-107 in newly diagnosed glioblastoma (GBM) patients. J Clin Oncol 32:15s, 2014 (suppl; abstr 2005).
18. Nair S, Archer GE, Tedder TF. Isolation and generation of human dendritic cells. Curr Protoc Immunol 2012;Chapter 7:Unit 7.32.
19. Mailliard RB, Wankowicz-Kalinska A, Cai Q, Wesa A, Hilkens CM, Kapsenberg ML, et al. alpha-type-1 polarized dendritic cells: a novel immunization tool with optimized CTL-inducing activity. Cancer Res 2004;64:5934–7.
20. Phuphanich S, Wheeler CJ, Rudnick JD, Mazer M, Wang H, Nuno MA, et al. Phase I trial of a multi-epitope-pulsed dendritic cell vaccine for patients with newly diagnosed glioblastoma. Cancer Immunol Immunother 2013; 62:125–35.
21. Jensen MM, Jorgensen JT, Binderup T, Kjaer A. Tumor volumein subcutaneous mouse xenografts measured by microCT is more accurate and reproducible than determined by 18F-FDG-microPET or external caliper. BMC Med Imaging 2008;8:16.
22. Tsai AK, Khan AY, Worgo CE, Wang LL, Liang Y, Davila E. A multikinase and DNA-PK inhibitor combination immunomodulates melanomas, suppresses tumor progression, and enhances immunotherapies. Cancer Immunol Res 2017;5:790–803.

23. Sanchez-Sanchez N, Riol-Blanco L, Rodriguez-Fernandez JL. The multiple personalities of the chemokine receptor CCR7 in dendritic cells. J Immunol 2006;176:5153–9.
24. Lee AW, Truong T, Bickham K, Fonteneau JF, Larsson M, Da Silva I, et al. A clinical grade cocktail of cytokines and PGE_2 results in uniform maturation of human monocyte-derived dendritic cells: implications for immunotherapy. Vaccine 2002;20 Suppl 4:A8–A22.
25. Koski GK, Koldovsky U, Xu S, Mick R, Sharma A, Fitzpatrick E, et al. A novel dendritic cell-based immunization approach for the induction of durable Th1-polarized anti-HER-2/neu responses in women with early breast cancer. J Immunother 2012;35:54–65.
26. Zhang JG, Eguchi J, Kruse CA, Gomez GG, Fakhrai H, Schroter S, et al. Antigenic profiling of glioma cells to generate allogeneic vaccines or dendritic cell-based therapeutics. Clin Cancer Res 2007;13:566–75.
27. Lopez-Cotarelo P, Escribano-Diaz C, Gonzalez-Bethencourt IL, Gomez-Moreira C, Deguiz ML, Torres-Bacete J, et al. A novel MEK-ERK-AMPK signaling axis controls chemokine receptor CCR7-dependent survival in human mature dendritic cells. J Biol Chem 2015;290:827–40.
28. Puig-Kroger A, Relloso M, Fernandez-Capetillo O, Zubiaga A, Silva A, Bernabeu C, et al. Extracellular signal-regulated protein kinase signaling pathway negatively regulates the phenotypic and functional maturation of monocyte-derived human dendritic cells. Blood 2001; 98:2175–82.
29. Goodwin JF, Knudsen KE. Beyond DNA repair: DNA-PK function in cancer. Cancer Discov 2014;4:1126–39.
30. Sato H, Niimi A, Yasuhara T, Permata TBM, Hagiwara Y, Isono M, et al. DNA double-strand break repair pathway regulates PD-L1 expression in cancer cells. Nat Commun 2017;8:1751.
31. Subramanian Vignesh K, Landero Figueroa JA, Porollo A, Caruso JA, Deepe GS Jr. Granulocyte macrophage-colony stimulating factor induced Zn sequestration enhances macrophage superoxide and limits intracellular pathogen survival. Immunity 2013;39:697–710.
32. Bauer M, Goldstein M, Christmann M, Becker H, Heylmann D, Kaina B. Human monocytes are severely impaired in base and DNA double-strand break repair that renders them vulnerable to oxidative stress. Proc Natl Acad Sci U S A 2011;108:21105–10.
33. Sallusto F, Cella M, Danieli C, Lanzavecchia A. Dendritic cells use macropinocytosis and the mannose receptor to concentrate macromolecules in the major histocompatibility complex class II compartment: downregulation by cytokines and bacterial products. J Exp Med 1995; 182:389–400.
34. Han TH, Jin P, Ren J, Slezak S, Marincola FM, Stroncek DF. Evaluation of 3 clinical dendritic cell maturation protocols containing lipopolysaccharide and interferon-gamma. J Immunother 2009;32:399–407.
35. Jin P, Han TH, Ren J, Saunders S, Wang E, Marincola FM, et al. Molecular signatures of maturing dendritic cells: implications for testing the quality of dendritic cell therapies. J Transl Med 2010;8:4.
36. Manavalan JS, Rossi PC, Vlad G, Piazza F, Yarilina A, Cortesini R, et al. High expression of ILT3 and ILT4 is a general feature of tolerogenic dendritic cells. Transpl Immunol 2003;11:245–58.
37. Penna G, Roncari A, Amuchastegui S, Daniel KC, Berti E, Colonna M, et al. Expression of the inhibitory receptor ILT3 on dendritic cells is dispensable for induction of CD4+Foxp3+ regulatory T cells by 1,25-dihydroxyvitamin D3. Blood 2005;106:3490–7.
38. Varga G, Balkow S, Wild MK, Stadtbaeumer A, Krummen M, Rothoeft T, et al. Active MAC-1 (CD11b/CD18) on DCs inhibits full T-cell activation. Blood 2007;109:661–9.
39. Maurya N, Gujar R, Gupta M, Yadav V, Verma S, Sen P. Immunoregulation of dendritic cells by the receptor T cell Ig and mucin protein-3 via Bruton's tyrosine kinase and c-Src. J Immunol 2014;193:3417–25.
40. Heufler C, Koch F, Stanzl U, Topar G, Wysocka M, Trinchieri G, et al. Interleukin-12 is produced by dendritic cells and mediates T helper 1 development as well as interferon-gamma production by T helper 1 cells. Eur J Immunol 1996;26:659–68.
41. Nogueira-Machado JA, Volpe CM, Veloso CA, Chaves MM. HMGB1, TLR and RAGE: a functional tripod that leads to diabetic inflammation. Expert Opin Ther Targets 2011;15:1023–35.
42. Mattei F, Schiavoni G. TIM-3 as a molecular switch for tumor escape from innate immunity. Front Immunol 2012;3:418.
43. Vermi W, Soncini M, Melocchi L, Sozzani S, Facchetti F. Plasmacytoid dendritic cells and cancer. J Leukoc Biol 2011;90:681–90.
44. Le Gall CM, Weiden J, Eggermont LJ, Figdor CG. Dendritic cells in cancer immunotherapy. Nat Mater 2018;17:474–5.
45. Rescigno M, Martino M, Sutherland CL, Gold MR, Ricciardi-Castagnoli P. Dendritic cell survival and maturation are regulated by different signaling pathways. J Exp Med 1998;188:2175–80.
46. Carter AB, Hunninghake GW.A constitutive active MEK → ERK pathway negatively regulates NF-kappa B-dependent gene expression by modulating TATA-binding protein phosphorylation. J Biol Chem 2000; 275:27858–64.
47. Aguilera-Montilla N, Chamorro S, Nieto C, Sanchez-Cabo F, Dopazo A, Fernandez-Salguero PM, et al. Aryl hydrocarbon receptor contributes to the MEK/ERK-dependent maintenance of the immature state of human dendritic cells. Blood 2013;121:e108–17.
48. Saikali S, Avril T, Collet B, Hamlat A, Bansard JY, Drenou B, et al. Expression of nine tumour antigens in a series of human glioblastoma multiforme: interest of EGFRvIII, IL-13Ralpha2, gp100 and TRP-2 for immunotherapy. J Neurooncol 2007;81:139–48.
49. Haynik DM, Roma AA, Prayson RA. HER-2/neu expression in glioblastoma multiforme. Appl Immunohistochem Mol Morphol 2007;15:56–8.
50. Iwami K, Shimato S, Ohno M, Okada H, Nakahara N, Sato Y, et al. Peptide-pulsed dendritic cell vaccination targeting interleukin-13 receptor alpha2 chain in recurrent malignant glioma patients with HLA-A*24/A*02 allele. Cytotherapy 2012;14:733–42.